




# Dissociative frustrated double ionization of N<sub>2</sub>Ar dimers in strong laser fields

Fenghao Sun<sup>1</sup>, Wenbin Zhang<sup>1</sup>, Peifen Lu<sup>1</sup>, Qiying Song<sup>1</sup> , Kang Lin<sup>1</sup>, Qinying Ji<sup>1</sup>, Junyang Ma<sup>1</sup>, Hanxiao Li<sup>1</sup>, Junjie Qiang<sup>1</sup>, Xiaochun Gong<sup>1</sup> , Hui Li<sup>1</sup> and Jian Wu<sup>1,2</sup> 

<sup>1</sup> State Key Laboratory of Precision Spectroscopy, East China Normal University, Shanghai 200062, People's Republic of China

<sup>2</sup> Collaborative Innovation Center of Extreme Optics, Shanxi University, Taiyuan, Shanxi 030006, People's Republic of China

E-mail: [jwu@phy.ecnu.edu.cn](mailto:jwu@phy.ecnu.edu.cn)

Received 24 September 2019, revised 28 October 2019

Accepted for publication 25 November 2019

Published 14 January 2020



## Abstract

We experimentally investigate the dissociative frustrated double ionization of N<sub>2</sub>Ar dimers exposed to strong laser fields by measuring the ejected charged and excited neutral Rydberg fragments in coincidence. The results show that the tunneled electron is more likely to be recaptured by the argon atomic ion than the nitrogen molecular ion to form the neutral Rydberg fragment in the dissociative frustrated double ionization of N<sub>2</sub>Ar dimers. It is attributed to the T-shaped molecular structure and the electron-localization-assisted enhanced ionization of the N<sub>2</sub>Ar dimer.

Keywords: Rydberg state, dissociative frustrated double ionization, femtosecond laser pulse

(Some figures may appear in colour only in the online journal)

## 1. Introduction

Strong-field ionization is one of the most fundamental processes for atoms and molecules exposed to intense laser fields. For the tunneling ionization, the bound electron is freed by surmounting the Coulombic potential barrier dressed by the laser field. Afterwards, the liberated electron driven by the oscillating laser field can either be released directly or re-collide with the parent ion. The recollision between the electron and its parent ion is responsible for many important strong-field phenomena, e.g. non-sequential double ionization [1, 2], high harmonic generation [3, 4], and laser-induced electron diffraction [5, 6]. Besides, there is another fate for the tunneled electron, i.e. being recaptured into highly excited Rydberg states. In a semi-classical picture, the electron that tunnels out near the maxima of the oscillating optical fields of a linearly polarized pulse gains near-zero drift momentum from the laser field so that it might be eventually recaptured into a Rydberg orbital by the Coulomb attraction of the parent ion core after the conclusion of the laser pulse. This phenomenon of electron recapture is denoted as frustrated tunneling ionization, which was initially observed in atoms exposed

to strong laser fields [7–10] and afterwards in molecules [11, 12] featured with rich dynamics [13–16].

In this paper, we focus on the dissociative frustrated double ionization (FDI) of the N<sub>2</sub>Ar dimer, which is composed of a covalent bond molecule and a rare gas atom with comparable ionization potential, to explore by which core the tunneled electron is prone to be recaptured. When the N<sub>2</sub>Ar dimer is exposed to strong laser fields, the van der Waals (vdW) bond can be broken up after the removal of two electrons, leading to the molecular ion N<sub>2</sub><sup>+</sup> being separated from the atomic ion Ar<sup>+</sup>. Despite the interaction between the molecular ion and the atomic ion, the electron recaptured by the molecular ion or the atomic ion was believed to be similar to the case of the isolated monomers. It was recently demonstrated that the N<sub>2</sub> and its companion atom Ar have comparable probabilities of the Rydberg state excitation in the single ionization of the corresponding monomers driven by intense 800 nm laser pulses [16]. However, the atom Ar and the molecule N<sub>2</sub> bound in a dimer show distinct features in the Rydberg state excitation driven by strong laser fields as compared with the isolated monomers. It was reported that the

tunneled electron prefers to be recaptured by the atomic ion in the triple or quadruple ionization of  $N_2Ar$  dimers [17] which was deduced from the kinetic energy release (KER) spectrum of the detected ionic fragments. Here, different to the previous experiment [17] focusing on the charged Rydberg states from the multiply ionized dimers, we experimentally investigate the dissociative FDI process of  $N_2Ar$  dimers where only one electron eventually escapes and the other electron is recaptured in neutral Rydberg states either by the atomic or molecular ions. Since only one electron from each core is initially released in the dissociative FDI process in contrast to the complex multiple ionization process, it is more straightforward to investigate the preference of the recapture of the tunneled electron in the dissociative FDI of  $N_2Ar$  dimers. By measuring the ejected Rydberg and ionic fragments in coincidence, we unambiguously identify the dissociative FDI channels for direct comparison, which is impossible in previous measurements based on the KER spectrum of the charged fragments.

## 2. Experiment

As schematically illustrated in figure 1(a), the measurements were performed in an ultrahigh-vacuum reaction microscope setup of COLd Target Recoil Ion Momentum Spectroscopy (COLTRIMS) [18, 19]. A linearly polarized femtosecond laser pulses beam (25 fs, 790 nm, 10 kHz) from a Ti:sapphire amplifier system was focused onto a supersonic gas jet by a concave silver mirror ( $f = 75$  mm) in the COLTRIMS. The dimers (about 2% with respect to the monomers) were generated by supersonic expanding the 1:1 mixture of  $N_2$  and Ar through a  $30 \mu\text{m}$  nozzle at a driving pressure of 1.5 bar. The temperature of the  $N_2$ -Ar dimer in the molecular beam was estimated to be about 4.8 K by using the equation of  $T_{\text{trans}} = \Delta p^2 / [4 \ln(4) k_B m]$  [20]. Here,  $k_B$  is the Boltzmann constant,  $\Delta p$  and  $m$  are the full-width at half-maximum (FWHM) of the momentum distribution (in the jet direction) and mass of singly ionized dimer. In our experiment the momentum width in the jet direction was measured to be  $\Delta p \sim 3.25$  a.u. for the  $N_2Ar^+$  ions created by a laser pulse linearly polarized along  $z$  direction (orthogonal to the gas jet). Besides the  $N_2Ar$  dimers, there were  $N_2-N_2$  and  $Ar_2$  dimers produced in the supersonic molecular beam. The laser intensity in the interaction zone was estimated to be  $1.4 \times 10^{15} \text{ W cm}^{-2}$  by tracing the intensity-dependent time-of-flight spectrum of protons from the dissociative ionization of  $H_2$  [21]. Three-dimensional momenta and thus the KERs of the ejected nuclear fragments were reconstructed according to the time-of-flight and positions of the impacts on the microchannel plate (MCP) detector during the offline analysis.

In our experiment, the produced ionic fragment ( $Ar^+$  or  $N_2^+$ ) can be accelerated by the static electric field of the spectrometer  $E_s$  ( $\sim 19.7 \text{ V cm}^{-1}$ ) and reach the ion detector regardless of its initial ejection direction, while the neutral Rydberg fragment ( $N_2^*$  or  $Ar^*$ ) can be detected only if it flies toward the detector [22]. It should be mentioned here the

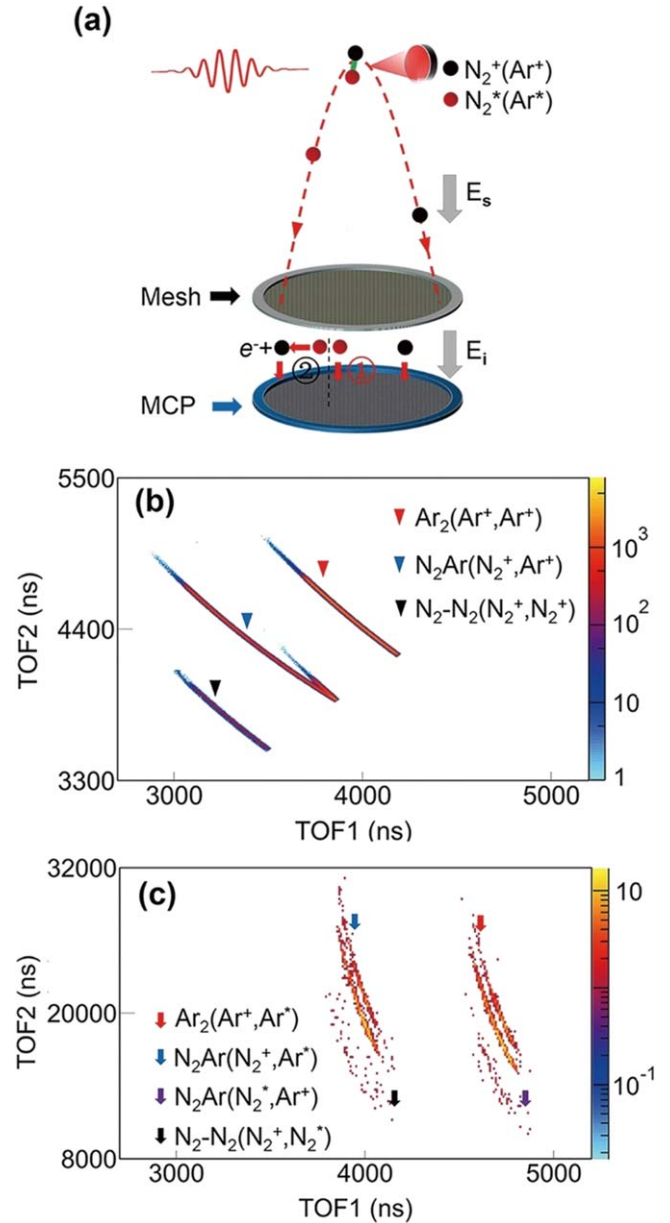


**Figure 1.** (a) Schematic illustration of the experimental setup. The neutral Rydberg fragment (red) survived from the field of the spectrometer  $E_s$  can be detected by the ion detector either as a neutral fragment (labeled as ①) or indirectly as an ionic fragment (labeled as ②) after the field ionization and acceleration by the electric field  $E_i$  between the mesh and MCP. (b) and (c) PIPICO spectra of the nuclear fragments from the Coulomb-exploded double ionization and from the dissociative frustrated double ionization of  $N_2Ar$  dimers as well as  $Ar_2$  and  $N_2-N_2$  dimers.

limited detection angle of the excited neutral fragments will lead to the underestimation of the electron recapture probability, but the detection solid angle for the excited neutral fragments is independent of the species. The detection solid angle is determined by the diameter of the MCP and the distance between the MCP and the focal spot of the laser beam, which was estimated to be  $0.9\pi$  Sr in the experiments [23]. Due to the low rate of the electron recapture events, the data presented here was accumulated for about 140 h with pump laser pulses of 10 kHz.

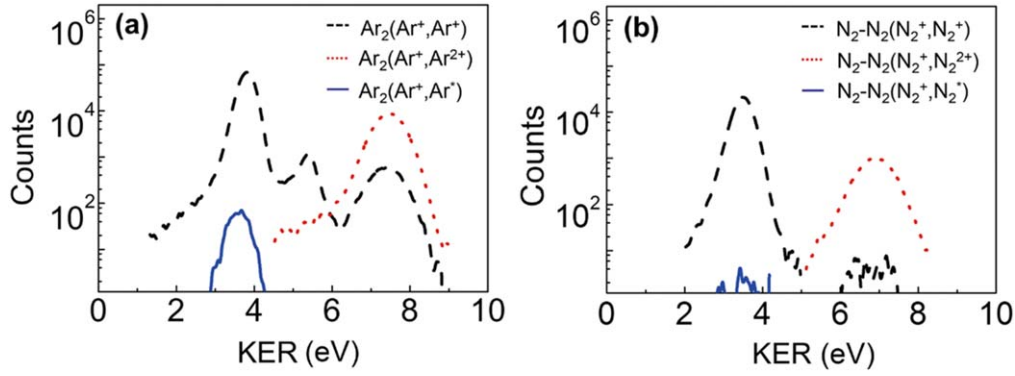


**Figure 2.** KER spectra of various two-body fragmentation channels of (a) the  $\text{Ar}_2$  dimers and (b) the  $\text{N}_2\text{-N}_2$  dimers.

### 3. Results and discussions

Figure 1(b) shows the photoion-photoion coincidence (PIPICO) spectrum of the ionic fragments from the Coulomb-exploded double ionization of  $\text{N}_2\text{Ar}$  dimers as well as  $\text{Ar}_2$  and  $\text{N}_2\text{-N}_2$  dimers irradiated by the linearly polarized laser pulses, i.e.  $\text{N}_2\text{Ar} + n\hbar\omega \rightarrow \text{N}_2^+ + \text{Ar}^+ + 2e$ ,  $\text{Ar}_2 + n\hbar\omega \rightarrow \text{Ar}^+ + \text{Ar}^+ + 2e$ , and  $\text{N}_2\text{-N}_2 + n\hbar\omega \rightarrow \text{N}_2^+ + \text{N}_2^+ + 2e$ , denoted as  $(\text{N}_2^+, \text{Ar}^+)$ ,  $(\text{Ar}^+, \text{Ar}^+)$  and  $(\text{N}_2^+, \text{N}_2^+)$ , respectively. During the Coulomb explosion process after the double ionization, one of the outgoing ionic fragments might be neutralized by recapturing a tunneled electron into the highly excited Rydberg states. In contrast to the charged fragment, the neutral fragment takes much longer time to reach the ion detector with the momentum merely gained in the dissociation since it cannot be accelerated by the electric field of the spectrometer [22]. For the dissociative FDI of  $\text{N}_2\text{Ar}$  dimers, there are two possible channels corresponding to the electron recapture by the molecular ion  $\text{N}_2^+$  and the atomic ion  $\text{Ar}^+$ , i.e.  $\text{N}_2^* + \text{Ar}^+ + e$  and  $\text{N}_2^+ + \text{Ar}^* + e$ , respectively denoted as  $(\text{N}_2^+, \text{Ar}^*)$  and  $(\text{N}_2^+, \text{Ar}^*)$ . As shown in figure 1(c), we identify the  $(\text{Ar}^+, \text{N}_2^*)$ ,  $(\text{Ar}^*, \text{N}_2^+)$ ,  $(\text{Ar}^+, \text{Ar}^*)$  and  $(\text{N}_2^+, \text{N}_2^*)$  fragment pairs from the dissociative FDI of the  $\text{N}_2\text{Ar}$ ,  $\text{Ar}_2$  and  $\text{N}_2\text{-N}_2$  dimers in the PIPICO spectrum of the nuclear fragments. In our experiment, the neutral Rydberg fragment can be detected by the ion detector either as a highly excited neutral fragment (denoted as direct Rydberg) or indirectly as an ion fragment after the static field ionization and acceleration by the electric field  $E_i$  ( $\sim 2022 \text{ V cm}^{-1}$ ) between the mesh and MCP (denoted as dc-ionized Rydberg), as illustrated in figure 1(a). This leads to the dual PIPICO lines for each dissociative FDI channel as displayed in figure 1(c), where the parallel low- and up-lines with small and large TOF2 are the dc-ionized and direct Rydberg fragments respectively.

Figure 2 depicts the measured KER spectra of various two-body fragmentation channels of  $\text{Ar}_2$  and  $\text{N}_2\text{-N}_2$  dimers. As shown in figure 2(a), there are three peaks in the KER spectrum (black dashed line) of the detected fragment pairs  $(\text{Ar}^+, \text{Ar}^+)$ , which is consistent with the previous experimental observation [24]. The first peak around 3.8 eV corresponds to the dissociative double ionization of  $\text{Ar}_2$  dimers, i.e. Coulomb explosion induced by peeling off two electrons. Meanwhile, one tunneled electron might be recaptured by one

of the two outgoing  $\text{Ar}^+$  fragments during the Coulomb explosion process, leading to the dissociative FDI channel of  $(\text{Ar}^+, \text{Ar}^*)$ . Accordingly, the KER spectrum (blue solid line) of the fragment pair  $(\text{Ar}^+, \text{Ar}^*)$  very well resembles the first peak of the KER spectrum of the fragment pair  $(\text{Ar}^+, \text{Ar}^+)$ . The KER of nuclear fragments of the FDI channel originating from the double ionization is much larger than that of the dissociation of the singly charged dimer. Here, we also present the KER spectrum (red dotted line) of the detected fragment pairs  $(\text{Ar}^+, \text{Ar}^{2+})$ , which is similar to the third peak of the KER spectrum of the fragment pair  $(\text{Ar}^+, \text{Ar}^+)$ . Analogously, it can be confirmed that the fragment pair  $(\text{Ar}^+, \text{Ar}^+)$  peaked around 7.3 eV comes from the dissociative frustrated triple ionization of  $\text{Ar}_2$  dimers, i.e. one tunneled electron is recaptured by the outgoing  $\text{Ar}^{2+}$  during the Coulomb explosion process after peeling off three electrons. Actually, the KERs of the charged Rydberg fragments observed in our experiments is in consistence with those presented in [17]. Similarly, for  $\text{N}_2\text{-N}_2$  dimers, as shown in figure 2(b), there also exists the electron recapture during the Coulomb explosion process after the double or triple ionization of  $\text{N}_2\text{-N}_2$  dimers. The recapture probabilities in the  $\text{N}_2\text{-N}_2$  dimers are much lower as compared to the  $\text{Ar}_2$  dimers.

In order to explore the ingredients in determining the probability that the tunneled electron gets recaptured into the Rydberg state, the relative recapture probabilities of various Rydberg channels are listed in table 1. The value of the recapture probability in table 1 is the yield ratio of the recapture channel to all the channels with the same initial charge state. For example, the relative recapture probability of the  $\text{N}_2\text{Ar}(\text{N}_2^+, \text{Ar}^*)$  channel is calculated by using the equation of

$$P_{\text{N}_2\text{Ar}(\text{N}_2^+, \text{Ar}^*)} = \frac{\text{Yield}(\text{N}_2\text{Ar}(\text{N}_2^+, \text{Ar}^*))}{\text{Yield}(\text{N}_2\text{Ar}(\text{N}_2^+, \text{Ar}^+)) + \text{Yield}(\text{N}_2\text{Ar}(\text{N}_2^+, \text{Ar}^*)) + \text{Yield}(\text{N}_2\text{Ar}(\text{N}_2^*, \text{Ar}^+))}$$

The numbers in the parentheses are the events of the dc-ionized Rydberg fragments of the corresponding channel, for which the influence of any difference of the detection efficiency of the MCP for the  $\text{N}_2^*$  and  $\text{Ar}^*$  will be removed. Both theory and experiment have proved that the dc-ionized neutral fragments of  $\text{N}_2^*$  and  $\text{Ar}^*$  have a similar response to the static field and obey

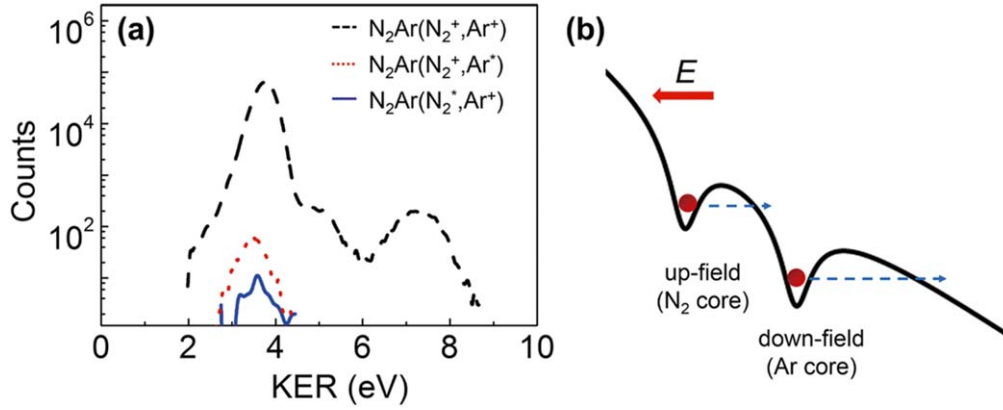


**Figure 3.** (a) KER spectra of the  $(N_2^+, Ar^+)$ ,  $(N_2^+, Ar^*)$  and  $(N_2^*, Ar^+)$  channels of the  $N_2Ar$  dimers. (b) The field-dressed double well potential of the  $N_2Ar^+$  dimer ion.

**Table 1.** Statistic data of various ionization-induced two-body fragmentation channels of the  $N_2Ar$ ,  $Ar_2$  and  $N_2-N_2$  dimers exposed to strong laser fields. The channels marked with “\*” come from the dissociative frustrated ionization, indicating that the tunneled electron is recaptured by an ionic fragment into a Rydberg state. The recapture probability is estimated by the event counts ratio of the recapture channel to all the channels with the same initial charge state. The numbers in the parentheses are the events of the dc-ionized Rydberg fragments of the corresponding channel.

Channels	KER (eV)	Event counts	Recapture probability (%)
$Ar_2(Ar^+, Ar^{2+})$	7.5	$176116 \pm 419$	
$Ar_2(Ar^+, Ar^{*+})$	7.3	$11396 \pm 107$	$6.08 \pm 0.06$
$Ar_2(Ar^+, Ar^+)$	3.8	$725482 \pm 852$	
$Ar_2(Ar^+, Ar^*)$	3.5	$895 (625 \pm 25)$	$0.086 \pm 0.003$
$N_2-N_2(N_2^+, N_2^{2+})$	6.9	$20415 \pm 143$	
$N_2-N_2(N_2^+, N_2^{*+})$	6.9	$128 \pm 11$	$0.62 \pm 0.06$
$N_2-N_2(N_2^+, N_2^+)$	3.5	$227511 \pm 477$	
$N_2-N_2(N_2^+, N_2^*)$	3.4	$54 (12 \pm 3)$	$0.005 \pm 0.001$
$N_2Ar(N_2^+, Ar^+)$	3.7	$688037 \pm 829$	
$N_2Ar(N_2^+, Ar^*)$	3.5	$779 (570 \pm 24)$	$0.083 \pm 0.004$
$N_2Ar(N_2^*, Ar^+)$	3.5	$75 (11 \pm 3)$	$0.0016 \pm 0.0005$

the saddle-point model of static field ionization  $F = Z^3/(9n^4)$  by incorporating the effect of a linear Stark shift, where  $Z$  represents the charge state [16, 25, 26]. The Rydberg fragments with quantum number  $n > 73$  will be ionized by the weak static electric field of  $E_s$  ( $\sim 19.7 \text{ V cm}^{-1}$ ) in the drift region of the spectrometer and arrive at the detector quickly, which are not included in the dual-line structure of the PIPICO spectrum of the dissociative FDI channels. On the other hand, the photon excitation created Rydberg fragments with quantum number  $n > 23$  will be ionized by the strong dc field ( $2022 \text{ V cm}^{-1}$ ) between the mesh and MCP and detected as charged ions (dc-ionized Rydberg). Thus, the principle quantum number of the dc-ionized Rydberg fragments, i.e. the low line of the dual PIPICO lines, in our experiment was estimated to be  $23 < n < 73$ . Overall, it can be seen that the tunneled electron is more likely to be recaptured by the ionic fragment with higher charge state after the triple ionization, which agrees well with the results of the previous studies [17, 24]. However, the electron recapture following the double ionization of  $N_2-N_2$ , i.e.

the dissociative FDI of  $N_2-N_2$ , is strongly suppressed as compared to  $Ar_2$ , although the Rydberg state excitation of the  $N_2$  monomer has a comparable probability as that of the  $Ar$  monomer in their frustrated single ionization [16].

We now examine the preference of electron recapture by the  $N_2^+$  or  $Ar^+$  in the dissociative FDI of the  $N_2Ar$  dimer. Figure 3(a) shows the KER spectra of the two-body fragmentation of the  $N_2Ar$  dimer. The first low-energy peak of the KER spectrum of the  $(N_2^+, Ar^+)$  fragment pair originates from the Coulomb explosion following the sequential double ionization of  $N_2Ar$ . On the other hand, the tunneled electron might be recaptured by either  $N_2^+$  or  $Ar^+$ , correspondingly resulting in the  $(N_2^*, Ar^+)$  or  $(N_2^+, Ar^*)$  fragment pairs. As shown in figure 3(a), the yield of  $(N_2^*, Ar^+)$  is much lower than that of  $(N_2^+, Ar^+)$  in the same measurement, indicating that the tunneled electron prefers to be recaptured by the atomic ion  $Ar^+$ . By comparing the molecular structures of  $N_2Ar$  and  $N_2-N_2$  dimers, it can be found that the molecular axis of  $N_2$  in these two species of dimers is perpendicular to the vdW bond, which might lead to the great suppression of the electron recapture by the molecular ion  $N_2^+$  in the dimer in contrast to the  $N_2^+$  in the monomer.

For the T-shaped  $N_2Ar$  [27], the molecular axis of  $N_2$  orients perpendicularly to the laser field when the vdW bond is parallel to the laser field. Thus, the first electron is more likely to be ejected from the  $Ar$  site as compared to the perpendicularly orientated  $N_2$  site with relatively higher ionization threshold [28]. After the first ionization step, the release of the second electron from the  $N_2Ar^+$  will be significantly enhanced by the mechanism of the electron-localization-assisted enhanced ionization [28–31]. As depicted in figure 3(b), the second electron is most likely to tunnel out from the up-field  $N_2$  site when the laser field points from  $Ar^+$  to  $N_2$ . Once the second electron is tunneled, it will be immediately accelerated by the remaining laser field along with the Coulomb explosion of the vdW bond of  $N_2Ar$ . The second electron gains a drift velocity in the oscillating optical field depending on the vector potential at the moment of ionization and subsequently is prone to be recaptured by the parallel propagating nuclear fragment due to the Coulomb attraction. Here, the  $Ar^+$  is more competitive in recapturing the electron, which flying along the same direction as the second electron, than the perpendicularly oriented  $N_2^+$  in the dissociative

FDI of  $N_2Ar$ . Therefore, as listed in table 1, the electron recapture probability of the  $Ar^+$  in the  $N_2Ar$  dimer (0.083%) is increased as compared to that of the  $Ar^+$  in the  $Ar_2$  dimer (0.043% for each  $Ar^+$ ). Although the statistics of the dissociative FDI channels is low due to the low probability of the electron recapture and the limited efficiency in generating dimers in the supersonic beam, the relative numbers of the measured events clearly present the trend of the relative recapture probabilities of different channels.



#### 4. Summary

In summary, we have experimentally investigated the strong-field induced dissociative FDI of  $N_2Ar$  dimers by measuring the ejected charged and neutral nuclear fragments in coincidence. It has been observed that the tunneled electron is more likely to be recaptured by the  $Ar^+$  than by the  $N_2^+$  following the double ionization of  $N_2Ar$ . By comparing the electron recapture of  $N_2^+$  in the dimers with  $N_2^+$  in monomer, we found that the great suppression of the electron recapture of  $N_2^+$  in the dissociative FDI of the dimers might be attributed to the molecular geometry, i.e. the axis of the  $N_2$  in the dimer is perpendicularly orientated when the vdW bond is parallel to the laser field. Our results indicate that the molecular structure of the dimer plays an important role in the selective recapture of the tunneled electron in strong-field dissociative FDI of  $N_2Ar$ .

#### Acknowledgments

We thank H Lv and S L Hu for helpful discussions. This work is supported by the National Key R&D Program of China (Grant No. 2018YFA0306303), the National Natural Science Fund (Grant Nos. 11704125, 11425416, 61690224, 11761141004, 11621404), the Shanghai Sailing Program (Grant No. 16YF1402900), and the 111 project of China (Grant No. B12024).

#### ORCID iDs

Qiyong Song  <https://orcid.org/0000-0001-8303-1889>  
 Xiaochun Gong  <https://orcid.org/0000-0002-4826-6049>  
 Jian Wu  <https://orcid.org/0000-0002-1318-2291>

#### References

- [1] Walker B, Sheehy B, DiMauro L F, Agostini P, Schafer K J and Kulander K C 1994 *Phys. Rev. Lett.* **73** 1227

- [2] Fittinghoff D N, Bolton P R, Chang B and Kulander K C 1992 *Phys. Rev. Lett.* **69** 2642
- [3] L'Huillier A and Balcou P 1993 *Phys. Rev. Lett.* **70** 774
- [4] Corkum P B 1993 *Phys. Rev. Lett.* **71** 1994
- [5] Zuo T, Bandrauk A D and Corkum P B 1996 *Chem. Phys. Lett.* **259** 313
- [6] Blaga C I, Xu J, DiChiara A D, Sistrunk E, Zhang K, Agostini P, Miller T A, DiMauro L F and Lin C D 2012 *Nature* **483** 194
- [7] Nubbemeyer T, Gorling K, Saenz A, Eichmann U and Sandner W 2008 *Phys. Rev. Lett.* **101** 233001
- [8] Wang B, Li X, Fu P, Chen J and Liu J 2006 *Chin. Phys. Lett.* **23** 2729
- [9] Eichmann U, Saenz A, Eilzer S, Nubbemeyer T and Sandner W 2013 *Phys. Rev. Lett.* **110** 203002
- [10] Larimian S *et al* 2017 *Phys. Rev. A* **96** 021403
- [11] Manschwetus B, Nubbemeyer T, Gorling K, Steinmeyer G, Eichmann U, Rottke H and Sandner W 2009 *Phys. Rev. Lett.* **102** 113002
- [12] McKenna J, Zeng S, Hua J J, Saylor A M, Zohrabi M, Johnson N G, Gaire B, Carnes K D, Esry B D and Ben-Itzhak I 2011 *Phys. Rev. A* **84** 043425
- [13] Li Q, Tong X M, Morishita T, Wei H and Lin C D 2014 *Phys. Rev. A* **89** 023421
- [14] Zimmermann H, Patchkovskii S, Ivanov M and Eichmann U 2017 *Phys. Rev. Lett.* **118** 013003
- [15] Piraux B, Mota-Furtado F, O'Mahony P F, Galstyan A and Popov Yu V 2017 *Phys. Rev. A* **96** 043403
- [16] Lv H, Zuo W, Zhao L, Xu H, Jin M, Ding D, Hu S and Chen J 2016 *Phys. Rev. A* **93** 033415
- [17] Xie X, Wu C, Liu H, Li M, Deng Y, Liu Y, Gong Q and Wu C 2013 *Phys. Rev. A* **88** 065401
- [18] Dörner R, Mergel V, Jagutzki O, Spielberger L, Ullrich J, Moshhammer R and Schmidt-Böcking H 2000 *Phys. Rep.* **330** 95
- [19] Ullrich J, Moshhammer R, Dorn A, Dörner R, Schmidt L P H and Schmidt-Böcking H 2003 *Rep. Prog. Phys.* **66** 1463
- [20] Wu J, Vredenburg A, Ulrich B, Schmidt L P H, Meckel M, Voss S, Sann H, Kim H, Jahnke T and Dörner R 2011 *Phys. Rev. A* **83** 061403
- [21] Alnaser A S, Tong X M, Osipov T, Voss S, Maharjan C M, Shan B, Chang Z and Cocke C L 2004 *Phys. Rev. A* **70** 023413
- [22] Zhang W *et al* 2017 *Phys. Rev. Lett.* **119** 253202
- [23] Zhang W *et al* 2019 *Nat. Commun.* **10** 757
- [24] Wu J, Vredenburg A, Ulrich B, Schmidt L P H, Meckel M, Voss S, Sann H, Kim H, Jahnke T and Dörner R 2011 *Phys. Rev. Lett.* **107** 043003
- [25] Ilkov F A, Decker J E and Chin S L 1992 *J. Phys. B: At. Mol. Opt. Phys.* **25** 4005
- [26] Ma J *et al* 2019 *Phys. Rev. A* **99** 023414
- [27] Wu J, Kunitski M, Schmidt L P H, Jahnke T and Dörner R 2012 *J. Chem. Phys.* **137** 104308
- [28] Wu J, Gong X, Kunitski M, Amankona-Diawuo F K, Schmidt L P H, Jahnke T, Czasch A, Seideman T and Dörner R 2013 *Phys. Rev. Lett.* **111** 083003
- [29] Zuo T and Bandrauk A D 1995 *Phys. Rev. A* **52** R2511
- [30] Seideman T, Ivanov M Y and Corkum P B 1995 *Phys. Rev. Lett.* **75** 2819
- [31] Gong X, Song Q, Ji Q, Pan H, Ding J, Wu J and Zeng H 2014 *Phys. Rev. Lett.* **112** 243001